LA-UR- 09-04129

Approved for public release;
distribution is unlimited.

Title:	Deuterium ordering in Laves phase deuteride YFe2D4.2
Author(s):	J. Ropka R. Černý V. Paul-Boncour Th. Proffen
Intended for:	J. Solid State Chemistry

Los Alamos
NATIONAL LABORATORY
EST. 1943

Form 836 (7/06)

Deuterium ordering in Laves phase deuteride $YFe_2D_{4.2}$

J. Ropka[1], R. Černý[1,*], V. Paul-Boncour[2] and Th. Proffen[3]

[1]Laboratory of Crystallography, University of Geneva, quai E.-Ansermet 24, CH-1211 Geneva, Switzerland
[2]CMTR, ICMPE, CNRS, 2 rue H. Dunant, 94320 Thiais Cedex, France
[3]Lujan Neutron Scattering Center, LANL, MS H805, Los Alamos, NM 87545, USA

*Corresponding author: Radovan.Cerny@cryst.unige.ch

Dedicated to Jim Richardson (IPNS, Argonne)

Abstract

The structure of Laves phase deuteride $YFe_2D_{4.2}$ has been investigated by synchrotron and neutron (*ToF*) powder diffraction experiments between 60 K and 370 K. $YFe_2D_{4.2}$ crystallizes below 323K in fully ordered monoclinic structure (s.g. *Pc*, $Z = 8$, $a = 5.50663(4)$, $b = 11.4823(1)$, $c = 9.42919(6)$ Å, $\beta = 122.3314(5)°$, $V = 503.765(3)$ Å^3 at 290K) containing 4 yttrium, 8 iron and 18 deuterium atoms. Most of D-D distances are within the precision of the diffraction experiment longer than 2.1 Å, the shortest ones are of 1.96 Å. Seven iron atoms from eight are coordinated by deuterium in a trigonal bipyramid, similar to that in $TiFeD_{1.95\text{-}2}$. The eights iron atom is coordinated by deuterium in a tetrahedral configuration. The iron coordination by deuterium, and iron-deuterium distances points to the importance of the directional bonding between iron and deuterium atoms. The lowering of crystal symmetry due to deuterium ordering occurs at much higher temperature than magnetic order, and is therefore one of the parameters which are at the origin of magnetic transition at lower temperatures.

Introduction

The deuterides of cubic (C15) Laves phases have been widely studied for the influence of deuterium absorption on their magnetic properties. YFe_2, which can absorb up to 5 H per formula unit (/f.u.), is particularly interesting owing to the large variety of crystal structures obtained at different hydrogen content [1-7]. These crystal structures are related to an ordering of hydrogen atoms into interstitial sites below an order-disorder temperature T_{OD}, which leads either to superstructures or to a distortion of the cubic C15 structure of the parent intermetallic. Above the ordering temperature, the hydrides preserve the symmetry of the cubic Laves phase structure with hydrogen distributed on 96*g* (Y_2Fe_2) and 32*e* (Y_1Fe_3) sites. Most of ordered crystal structures of the corresponding deuterides, including the position and occupation factor of deuterium atoms, were characterized [5], with the exception of $YFe_2D_{1.9}$ and $YFe_2D_{4.2}$ which show a low symmetry and very large number of possible hydrogen interstitial sites.

$YFe_2D_{4.2}$ crystallizes above the deuterium ordering temperature $T_{OD} = 343$ K in the cubic structure (*Fd*-3*m*, $a = 7.95$ Å), between 323-343 K it shows a rhombohedral distortion (*R*-3*m*, $a = 5.702$ Å, $c = 12.404$ Å), and below 323 K down to 2 K in a monoclinic superstructure [7]. The monoclinic superstructure was described [8] in s. g. $P2_1/a$ with cell parameters $a = 9.399(3)$, $b = 5.740(3)$, $c = 5.494(3)$ Å, $\beta = 122.22(3)°$ which contains 11

partly occupied deuterium sites. Closer examination of the neutron powder patterns showed the existence of additional lines which could be indexed by doubling the cell parameter *b*. This lowering of the crystal symmetry can be described in the monoclinic space group $P1a1$ (in standard setting Pc when interchanging lattice parameters *a* and *c*). However, no attempt was done to solve the structure in the doubled cell so far due to the large number of possible interstitial sites for D atoms (64) and, therefore of atomic positions and occupancy factors to refine (256). A similar monoclinic superstructure was observed at 290 K in deuterium less rich phase $YFe_2D_{3.5}$ [9]. It derives from the same average monoclinic cell with parameters a = 9.482, b = 5.633, c = 5.494 Å, β = 123.84° by keeping the parameters *a* and *b*, and third parameter being the doubled face diagonal $a + c$. The structure was refined in the symmetry $P2_1/a$ resulting in 15 disordered deuterium positions with short D-D contacts.

The YFe_2D_x deuterides are ferromagnets with decreasing Curie temperature with x for $0 \leq x \leq 3.5$ [10]. YFe_2D_5 is a weak ferromagnet, without ordered Fe moments [6]. The intermediate phase between $3.5 < x < 5$, $YFe_2D_{4.2}$, undergoes at the transition temperature at zero field T_{MO} = 84 K a sharp magnetostrictive transition [7] corresponding upon heating to a transition from a ferromagnetic (F) to an antiferromagnetic (AF) structure characterized by a doubling of the magnetic cell along the *b*-axis [8]. The Néel temperature T_N, corresponding to the disappearance of the AF lines in the neutron powder diffraction pattern (NPD), is located at 131 K [7]. Above this temperature the compound is paramagnetic (P). The F-AF magnetic transition is strongly dependent of the applied magnetic field, and presents an itinerant electron metamagnetic behaviour. A volume decrease of 0.55 % was also observed at the transition from F to AF state [8]. In addition, a giant magnetic isotope effect is observed for the $YFe_2(D_yH_{1-y})_{4.2}$ as T_{MO} is shifted from 84 K for y = 0 to 112 K for y = 0.64 and 131 K for y = 1 [11]. This isotope effect was partly attributed to the high sensitivity of the magnetic transition to the difference of volume (0.8 %) observed between the hydride and the deuteride.

In this paper we will give the complete description of the monoclinic crystal structure of $YFe_2D_{4.2}$ between 290 K and 60 K. The localization of the D atoms is particularly important to analyze the Fe atom environments and to understand more clearly the origin of the F-AF transition, and the associated strong isotope effect. The magnetic structure of the AF phase, and the local order of deuterium atoms around the iron studied by the Pair Distribution Function analysis of the diffuse intensity in neutron powder pattern will be communicated separately.

Experimental

The YFe_2 intermetallic compound was prepared by induction melting of the pure elements followed by 3 weeks annealing treatment at 1100 K. The composition and homogeneity was checked by X-ray powder diffraction (XPD) and electron probe microanalysis (EPMA) as described in [7]. The $YFe_2D_{4.2}$ deuteride was prepared by solid-gas reaction using a Sievert apparatus and it homogeneity was checked by (XPD). Two samples were independently prepared by this protocol, and will be called as sample no. 1 and 2.

X-ray powder diffraction (XPD) measurements were carried out using a Bruker D8 diffractometer (Cu K_α radiation). Several synchrotron powder patterns (SPD) were collected on the sample no. 2 at Swiss-Norwegian Beam Line BM1B of the ESRF, Grenoble, France, to follow the temperature dependence of lattice parameters. The powder sample was closed in a 0.5 mm glass capillary, and the temperature was controlled with a special He-cryostat. Diffraction patterns (λ = 0.40001 Å) were collected with 6-crystals analyzer detector.

The time-of-flight (*ToF*) neutron powder data were collected at the GPPD spectrometer at the IPNS, Argonne National Laboratory (sample 1, T=290, 350, 370 K), and at the NPDF spectrometer at the LANSCE, Los Alamos National Laboratory (sample 2, T=60,

96, 200, 290 K), USA. The sample (7.7 g of sample no. 1, and 4.8 g of sample no. 2) was closed in a vanadium container, and the temperature was controlled by the Displex attachment.

The crystal structure was solved by the global optimization of the positions of deuterium atoms in the elementary cell (*Pc*) with the help of the program Fox [12]. The profile matching using the synchrotron data was done with the program FullProf [13]. The Rietveld refinement using the *ToF* data was done with the program GSAS [14].

Results

Lattice

The monoclinic *Pc* phase is observed at low temperatures starting from 290 K, in agreement with [7]. The variation of the volume/8 f.u. of $YFe_2D_{4.2}$ (= monoclinic cell volume) with the temperature as obtained on both samples and from different diffraction experiments is given in the Figure 1. It shows the effect of the magnetic phase transition at T_{MO} = 84 K and of deuterium ordering at T_{OD} = 343 K. A sharp volume increase is observed at the AF to F transition. The volume is also bigger in the deuterium disordered cubic phase as compared to the P monoclinic phase. Variation of monoclinic lattice parameters with temperature is given in the Figure 2. The "monoclinic" lattice parameters at 350 and 370 K are calculated from the cubic lattice of the disordered $YFe_2D_{4.2}$ phase according to the Eq. 1 given in the dicussion. In a similar way the volume/8 f.u. of $YFe_2D_{4.2}$, and "monoclinic" lattice parameters of the rhombohedral phase at 333 K were calculated from the reported data [8], and are shown in the Figure 1 and 2 too. In agreement with [7] the monoclinic lattice parameters show strong anisotropy (*b*-parameter increases) of the lattice contraction at deuterium ordering and a weak anisotropy (all parameters increase) of the lattice expansion due to the magnetoelastic effect at the transition from AF to F magnetic order. The volume decrease between 96 and 60 K as observed on sample no. 2 is 0.653 %. The magnetoelastic effect is less pronounced along the *b*-axis. The thermal dilatation is also strongly anisotropic, weaker along the *b*-axis, and stronger along the *a*- and *c*-axes, and shows anomaly when approaching the magnetic phase transition temperature T_{MO}.

Structure

When solving the crystal structure from *ToF* neutron data we have used 290 K data of the sample no. 1. The positions of metal atoms of $YFe_2D_{4.2}$ as described in the space group $P2_1/a$ [8] were transformed to the space group $P1a1$ with twice bigger cell volume ($b_{Pa} = 2b_{P21/a}$). This model with metal atoms fixed was used as a starting configuration for the localization of deuterium atoms using neutron data measured at 290 K where no contribution of magnetic peaks is observed. For the Rietveld refinement using the data at 96 and 60 K we have excluded the strongest magnetic peaks in the spectra (d=4.63 Å for F ordering and d=23.5, 5.51 and 3.98 Å for AF ordering). The contribution of other magnetic peaks was considered as negligible. The $YFe_2D_{4.2}$ structure was finally solved in the space group $P1c1$ with 12 independent metal atoms (Y on four sites 2*a* and Fe on eight sites 2*a*), and 18 deuterium atoms on sites 2*a*. The atomic parameters at 290 K refined on the sample no. 1 are given in Supporting Information (Table S1a). The coordination of yttrium and iron atoms by deuterium atoms is given in the Table S2. The refined composition is $YFe_2D_{4.27(5)}$. Traces of disordered cubic phase with the lattice parameter a = 7.9198(1) Å, and refined composition $YFe_2D_{4.54(4)}$ were observed in *ToF* data at 290 K. Its weight fraction as refined from the Rietveld refinement was 4.0(1)%.

The Rietveld refinement of the disordered phase at 350 and 370 K showed the cubic structure of the Laves phase deuteride with preferentially occupied 96*g* site by deuterium, less occupied 32*e* site and nearly empty 8*b* site in agreement with [8]. Further heating of the

sample to 400 K has resulted to a partial desorption of deuterium and decrease of the cell volume and refined deuterium content. The atomic parameters at 350 K refined on the sample no. 1 are given in the Supporting Information (Table S1b). The refined composition $YFe_2D_{4.65(2)}$ is higher than the refined composition of the ordered monoclinic phase at 290 K. The refinement agreement factors, especially R_{Bragg}, are also higher compared to the refinement at 290K. The same discrepancy was observed also at 370 K. The discrepancy between refined deuterium content in the same sample in ordered and disordered state can be understood as a result of wrong treatment of the diffuse intensity in the Rietveld refinement of the disordered phase. Very strong diffuse intensity due to short range correlations D-D is observed in all neutron powder patterns of $YFe_2D_{4.2}$ in disordered state. As Rietveld refinement ignores this observation, it results in a wrong estimation of the deuterium content in the sample, in our case to its overestimation, and to higher agreements factors. The same overestimation of the deuterium content by the Rietveld refinement was observed in the rhombohedral phase [8], which is not fully ordered, and shows the similar preference for the site occupation by deuterium as the cubic phase with even stronger preference for the three available Y_2Fe_2 sites to two Y_1Fe_3 sites.

The temperature dependent *ToF* data from the sample no. 2 resulted in the same structural parameters at 290 K as the sample no. 1. The *ToF* data measured on the sample no. 2 at 200, 96 and 60 K does not show any structural transition or modification which could be at the origin of the magnetic transitions (see essential interatomic distances and coordination in Table 1.).

The Rietveld plot of three data banks at 290 K from the GPPD diffractometer are shown in the Figure S1, and of three data banks at 96 K from the NPDF diffractometer are shown in the Figure S2 of the Supporting Information. The Crystallographic Information Files (CIF) of all refined structures are included too.

Discussion

Symmetry of the monoclinic phase

$YFe_2D_{4.2}$ at 290 K is an ordered phase in the monoclinic cell (s.g. *Pc*, $Z = 8$, $a = 5.50663(4)$, $b = 11.4823(1)$, $c = 9.42919(6)$ Å, $\beta = 122.3314(5)°$, $V = 503.765(3)$ Å^3). A relation between the lattice vectors of the cubic disordered and monoclinic ordered $YFe_2D_{4.2}$ is

$$\begin{aligned} \vec{a}_M &\approx \frac{1}{2}(\vec{a}_C + \vec{b}_C) \\ \vec{b}_M &\approx (\vec{a}_C - \vec{b}_C) \\ \vec{c}_M &\approx -\frac{1}{2}(\vec{a}_C + \vec{b}_C + 2\vec{c}_C) \end{aligned} \qquad (1)$$

where $\vec{a}_M, \vec{b}_M, \vec{c}_M$ are lattice vectors of the ordered monoclinic and $\vec{a}_C, \vec{b}_C, \vec{c}_C$ of the disordered cubic phase. The group-subgroup relation between the space group of the disordered phase *Fd-3m* and ordered phase *Pc* was analyzed with the help of the program SUBGROUPGRAPH [15]. Index of transformation is 96 and there exist a great number of possible chains between both space groups. However, taking into account that $YFe_2D_{4.2}$ structure is cubic in disordered state at high temperature, and changes its symmetry through the rhombohedral to the monoclinic [7] as temperature is decreasing only one chain of group-subgroup relations can be selected (Figure 5).

Atomic coordination

At 290 K all D-D distances are within the precision of the diffraction experiment longer than 2.1 Å, except D4-D11 (1.96 Å). If all deuterium sites were fully occupied the composition would be $YFe_2D_{4.5}$. It is worth to note that both samples were not fully saturated, but the refined composition of both samples was close to $YFe_2D_{4.2}$, and it justifies calling the phase by this formula. From 18 independent deuterium sites 15 corresponds to the 96*g* site (Y_2Fe_2) in the cubic space group *Fd*-3*m* of the disordered phase, and 3 to the 32*e* site (Y_1Fe_3). An interesting feature of the structure is the coordination of the iron atoms by deuterium (Table S2). Seven iron atoms are coordinated by a trigonal bipyramid, angle D-Fe-D for two apical deuterium atoms is in the range 166.1(4)-178.1(4)°, and angle D-Fe-D for two equatorial deuterium atoms is in the range 102.2(3)-147.5(4)°. Atom Fe1 is coordinated by a tetrahedron with tetrahedral angles within 100.9(3)-122.0(5)°. The Fe-D distances are within 1.618(7)-1.875(8) Å, and the shortest ones are close to the iron deuterium distances of 1.556 Å in the Mg_2FeD_6 deuteride [16] containing octahedral 18-electrons complexes $[FeD_6]^{-4}$. It points to the importance of the directional bonding between iron and deuterium atoms in $YFe_2D_{4.2}$. The increased importance of Fe-D bonding in $YFe_2D_{4.2}$ compared to deuterium less-rich deuterides of YFe_2 was shown in [17]. However, the coordination polyhedra FeD_x in $YFe_2D_{4.2}$ share all D-vertices and cannot be considered as 18-electron complexes. No FeD_5 or FeD_4 complexes are reported so far, and no ionic limiting formula can be written for $YFe_2D_{4.2}$. In spite of that we prefer the Fe-D polyhedral description of the structure to a description as an interstitial deuteride in the following discussion. The question whether the same order of deuterium around the iron atoms exists locally also in the disordered phase above T_{OD} = 343 K will be treated in a separate paper.

Similar trigonal bipyramidal coordination of iron by deuterium sharing also all vertices was found in monoclinic $TiFeD_2$ [18] and orthorhombic $TiFeD_{1.95}$ [19]. The Fe-D distances are within 1.65(1)-1.97(1), slightly longer than in $YFe_2D_{4.2}$. The angle D-Fe-D for two apical deuterium atoms is in the range 164.4(7)-167.0(7)°, and angle D-Fe-D for two equatorial deuterium atoms is in the range 92.2(1)-133.1(1)°, showing slightly more deformed trigonal bipyramid in $TiFeD_{1.95-2}$. Contrary to $YFe_2D_{4.2}$ the interstitial sites in $TiFeD_{1.95-2}$ occupied by deuterium are octahedral sites of the composition either Ti_2Fe_4 or Ti_4Fe_2.

Deuterium ordering vs. magnetic order

Band structure calculations on YFe_2H_x have shown that the increase of the cell volume due to increasing hydrogen content stabilizes the ferromagnetic structure with a raise of the Fe moment, whereas the increase of the number of Fe-H bonding tend to reduce the Fe moment until it become non stable in YFe_2H_5 [20, 21]. The magnetic properties of the YFe_2 hydrides (deuterides) results therefore from a competition between volume and electronic change induced by the insertion of H(D) atoms. The AF state$YFe_2H_{4.2}$ between T_{MO} = 84 K and T_N = 131 K was related [11] to the behaviour of the magnetic moment of one iron atom coordinated by more deuterium atoms than other iron atoms. Our results do not show such iron between 60 and 290 K. In the average structural model of the monoclinic phase in $P2_1/a$ [8] such iron was observed as coordinated by ~5 D atoms contrary to all other iron atoms coordinated by ~4 D atoms. It turned out that this model was only a projection of the true *Pc* model to the cell of half volume.

As it is shown in the left part of the Figure 3 the structure of the monoclinic $YFe_2D_{4.2}$ can be built up from the (20-1) layers containing Fe2-Fe7D_5 trigonal bypiramids. The layers are then stacked in the direction [-101] and connected by Fe1D_4 tetrahedron and Fe8D_5 trigonal bipyramid as shown in the Figure 4. These layers are equivalent to {111} layers of the disordered cubic structure of the Laves phase deuteride (Figure 3, right). This description follows the lowering of the symmetry in the transition cubic-rhombohedric-monoclinic

symmetry on cooling as the cubic {111} planes are the basal planes of the hexagonal lattice of the rhombohedral phase. On full ordering of deuterium atoms below 323 K in the monoclinic phase, these planes loose the hexagonal symmetry and expand along the b_M direction and contract along the perpendicular direction. The thermal dilatation as observed in the monoclinic phase is the weaker within the (20-1) layers (along the *b*-axis) and stronger in the direction perpendicular to the layers (along the *a*+*c* direction).

Another feature of this description is the particular position of Fe1, Fe6 and Fe8 atoms, which are less (Fe1) or slightly less (Fe6 and Fe8) coordinated by deuterium than all the other iron atoms (Table 1.). The position of Fe6 in the layer can be at the origin of the doubling of the AF cell in the *b*-direction. However, the origin of the observed AF order stays to be understood. Band structure calculations will be performed, using the results of the present work, in order to get a better understanding of the influence of the structural distortion and of the Fe-D bonding on the magnetic properties.

The monoclinic superstructure of the deuterium less rich phase $YFe_2D_{3.5}$ [9] is not fully ordered, and cannot be therefore easily related to the fully ordered $YFe_2D_{4.2}$. Both superstructures are created by doubling the periodicity of the common monoclinic sub-cell, but in different directions. The volume/f.u. is smaller in $YFe_2D_{3.5}$ (60.9 Å^3) than in $YFe_2D_{4.2}$ (62.9 Å^3), as expected from the lower deuterium content. The cell expansion due to deuterium content is, however, anisotropic: the parameter *a* (in the common monoclinic sub-cell) is longer in $YFe_2D_{3.5}$ (9.482 Å) than in $YFe_2D_{4.2}$ (9.429 Å). Whether $YFe_2D_{3.5}$ becomes fully ordered at lower temperatures, stays to be investigated.

Conclusions

The deuterium atoms in $YFe_2D_{4.2}$ are fully ordered from 290 down to 2 K in the monoclinic cell (s.g. *Pc*, a = 5.50663(4), b = 11.4823(1), c = 9.42919(6) Å, β = 122.3314(5)°, V = 503.765(3) Å^3 at 290K). The structural refinement shows that ten from eighteen deuterium sites are partly occupied, however, their occupancies are close to 90%. The saturated deuteride with all sites fully occupied would reach the composition $YFe_2D_{4.5}$. The D atoms occupy mainly A2B2 sites and most of the D-D distances are longer than 2.1 Å, the shortest one is of 1.96 Å. Seven Fe atoms are coordinated by deuterium in a trigonal bipyramid, similar to that in $TiFeD_{1.95-2}$,whereas the eights one is coordinated in a tetrahedral configuration. The same structure is maintained at 200, 96 and 60 K. A jump of the cell volume is observed at the AF-F transition. The deuterium ordering, which occurs at much higher temperature than magnetic order, is one of the parameters which are at the origin of AF and F ordering at lower temperatures.

Acknowledgements

We would like to thank to Hyunjeong Kim (Lujan Center) for the help with ToF data collection, and to Herman Emmerich (SNBL, ESRF Grenoble) for the help with the synchrotron data collection. The help of Yaroslav Tokaychuk (University of Geneva) with the sample synthesis is highly appreciated. This work has benefited from the use of NPDF at the Lujan Center at Los Alamos Neutron Science Center, funded by DOE Office of Basic Energy Sciences. Los Alamos National Laboratory is operated by Los Alamos National Security LLC under DOE Contract DE-AC52-06NA25396. The upgrade of NPDF has been funded by NSF through grant DMR 00-76488. The work was supported by the Swiss National Science Foundation.

References

[1] K.H.J. Buschow, A.M. Van Diepen, *Sol. State Comm.*, **19**(1) (1976) 79-81.
[2] V.V. Burnasheva, E.E. Fokina, S.L. Troitskaya, K.N. Semenenko, *Russian Journal of Inorganic Chemistry*, **29**(6) (1984) 792-794.
[3] K. Kanematsu, *J. Appl. Phys.*, **75**(10) (1994) 7105-7107.
[4] K. Kanematsu, N. Ohkubo, K. Itoh, S. Ban, T. Miyajima,Y. Yamaguchi, *J. Phys. Soc. Jap.*, **65**(4) (1996) 1072-1076.
[5] V. Paul-Boncour, L. Guénée, M. Latroche, A. Percheron-Guégan, B. Ouladdiaf, F. Bourée-Vigneron, *J. Solid State Chem.* **142** (1999) 120-129.
[6] V. Paul-Boncour, S.M. Filipek, A. Percheron-Guégan, I. Marchuk, J. Pielaszek, *J. Alloys and Compounds* **317–318** (2001) 83–87.
[7] V. Paul-Boncour, G. André, F. Bourée, M. Guillot, G. Wiesinger, A. Percheron-Guégan, *Physica B* **350** (2004) e27–e30.
[8] V. Paul-Boncour, M. Guillot, G. André, F. Bourée, G. Wiesinger, A. Percheron-Guégan, *J. Alloys and Compounds* **404–406** (2005) 355–359.
[9] G.Wiesinger, V. Paul-Boncour, S.M. Filipek, Ch. Reichl, I.Marchuk, A. Percheron-Guégan; *J. Phys.: Condens. Matter* **17** (2005) 893–908.
[10] V. Paul-Boncour, A. Percheron-Guégan, *J. Alloys and Compounds* **293–295** (1999) 237–242.
[11] V. Paul-Boncour, M. Guillot, G. Wiesinger, G. André, *Phys. Rev. B* **72** (2005) 174430.
[12] V. Favre-Nicolin, R. Černý, *J. Appl. Cryst.* **35** (2002) 734-743.
[13] J. Rodriguez-Carvajal, *Physica B.* **192** (1993) 55
Remarks:
For a more recent version see Rodríguez-Carvajal, J. Recent Developments of the Program FULLPROF, in Commission on Powder Diffraction (IUCr).
Newsletter (2001), 26, 12-19. (http://journals.iucr.org/iucr-top/comm/cpd/Newsletters/)
The complete program and documentation can be obtained at
http://www.ill.fr/dif/Soft/fp/
[14] A.C. Larson, R.B. Von Dreele, ***General Structure Analysis System (GSAS)***, Los Alamos National Laboratory Report LAUR 86-748 (2004).
[15] S. Ivantchev, E. Kroumova, G. Madariaga, J.M. Perez-Mato, M.I. Aroyo, *J. Appl. Cryst.* **33** (2000) 1190-1191.
[16] J.-J. Didisheim, P. Zolliker, K. Yvon, P. Fischer, J. Scheffer, M. Gubelmann, A.F. Williams, *Inorg. Chem.* **23** (1984) 1953-1957.
[17] V. Paul-Boncour, S.F. Matar, *Phys. Rev. B* **70** (2004) 184435.
[18] W. Schaefer, G. Will, T. Schober, *Materials Research Bulletin* **15** (1980) 627-634.
[19] P. Fischer, J. Schefer, K. Yvon, L. Schlapbach, T. Riesterer, *J. Less-Common Metals* **129** (1987) 39-45.
[20] D.J. Singh, M. Gupta, *Phys. Rev. B*, **69** (2004) 132403.
[21] J.C. Crivello, M. Gupta, *J. Alloys and Compounds*, **404-406** (2005) 150-154.

Table 1. First neighbors interatomic distances [Å] and deuterium coordination if iron atoms in $YFe_2D_{4.2}$ as refined from the neutron *ToF* data as a function of the temperature, sample no. 2.

Temperature [K]		***290***	***200***	***96***	***60***
Fe-D	*max*	1.84	1.90	1.83	1.84
	min	1.62	1.58	1.62	1.61
	av	1.72	1.72	1.72	1.73
CN Fe1		**3.82**	**3.61**	**3.81**	**3.84**
CN Fe6		**4.36**	**4.38**	**4.53**	**4.42**
CN Fe8		**4.32**	**4.54**	**4.47**	**4.40**
CN Fe	**(without Fe6,Fe8)**	**4.67**	**4.71**	**4.76**	**4.80**
Y-D	*max*	2.62	2.43	2.43	2.43
	min	2.12	2.13	2.14	2.13
	av	2.25	2.25	2.24	2.25
Fe-Fe	*max*	3.00	3.00	2.98	3.00
	min	2.67	2.71	2.67	2.68
	av	2.81	2.81	2.81	2.82
Y-Y	*max*	3.56	3.49	3.49	3.51
	min	3.36	3.37	3.37	3.38
	av	3.45	3.44	3.44	3.45

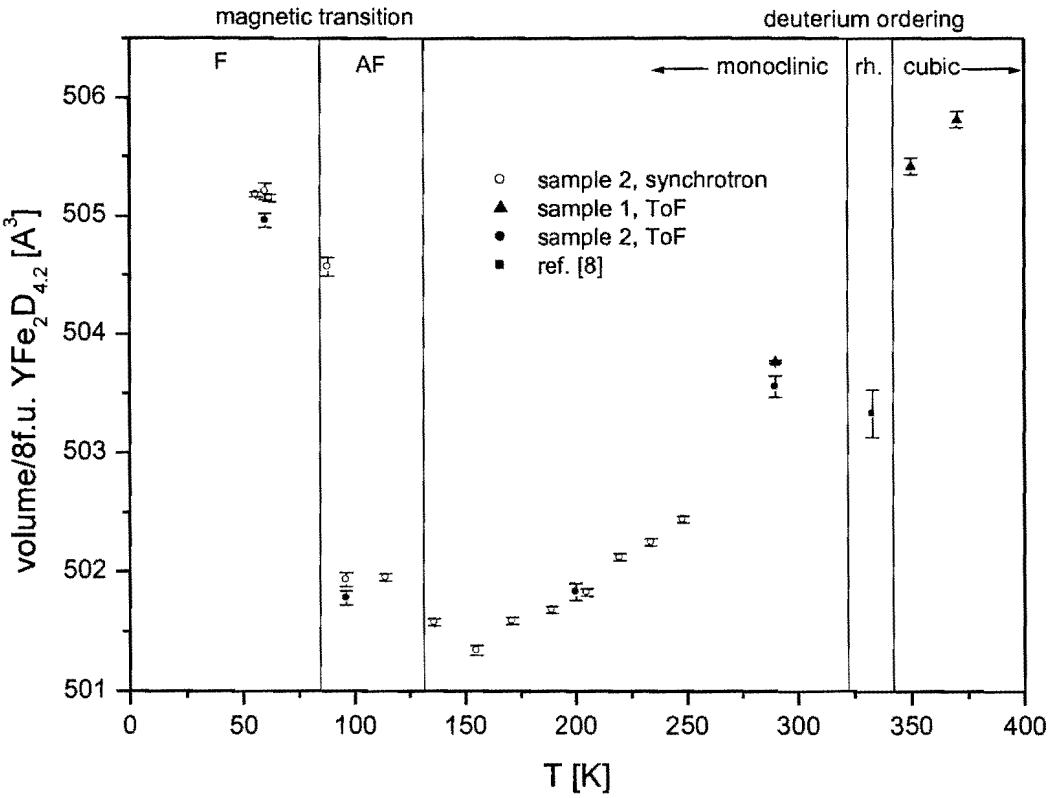

Figure 1: Temperature dependence of the volume/8 f.u. $YFe_2D_{4.2}$ (= monoclinic cell volume) from different powder diffraction experiments. Decrease of 0.653 % is observed at the transition from ferromagnetic (F) to antiferromagnetic (AF) phase. Similar volume increase is observed at the transition from ordered monoclinic to disordered cubic phase separated by the region of rhombohedraly distorted phase (rh.) as observed in [8].

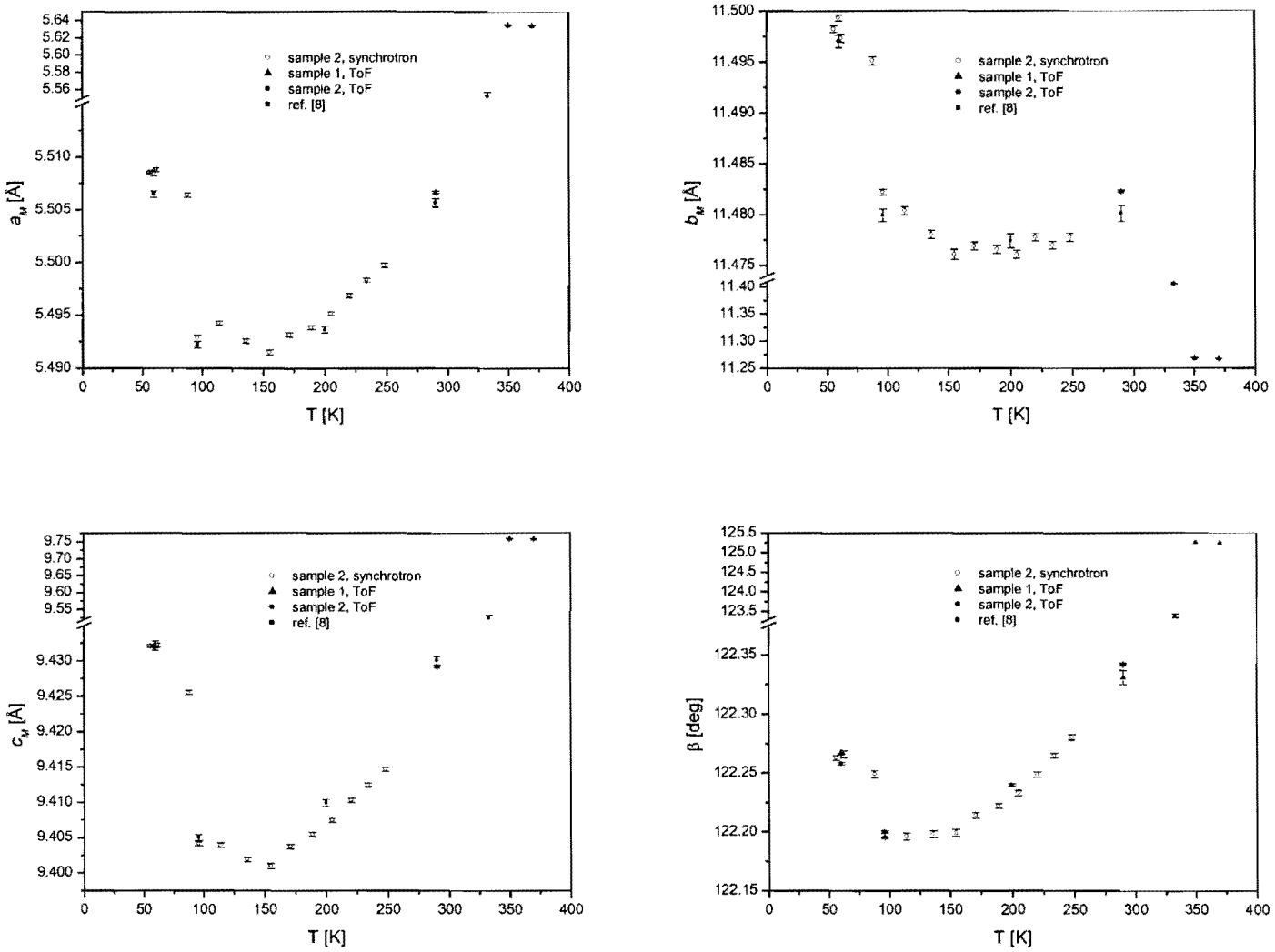

Figure 2: Temperature dependence of the monoclinic lattice parameters of $YFe_2D_{4.2}$ from different powder diffraction experiments showing strong anisotropy (*b*-parameter increases) of the lattice contraction at deuterium ordering and a weak anisotropy (all parameters increase) of the lattice expansion at the transition from AF to F magnetic order. The "monoclinic" lattice parameters at 333, 350 and 370 K are calculated by the transformation from the rhombohedric and cubic lattices.

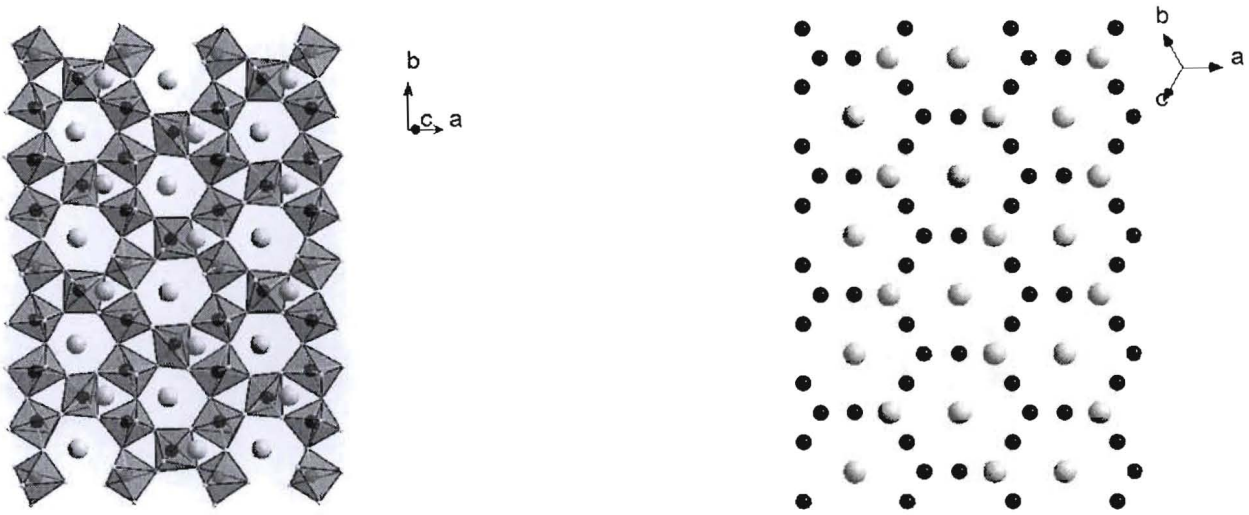

Figure 3: One layers (20-1) of the monoclinic $YFe_2D_{4.2}$ (left) equivalent to the close packed planes {111} of the cubic structure (right, only metal atoms are shown, Y light, Fe dark), as a basic building unit of the monoclinic structure built up from Fe2-Fe7D_5 trigonal bypiramids and viewed along [-101], Fe6 in red.

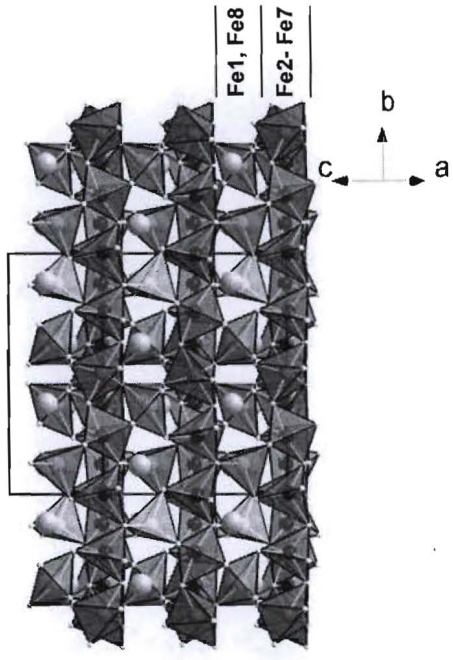

Figure 4: Structure of the monoclinic $YFe_2D_{4.2}$ as built up from the (20-1) layers (3 layers are shown) viewed along [201]. The layers are connected in the [-101] direction by Fe1D_4 tetrahedra and Fe8D_5 trigonal bipyramids, Fe1 in blue, Fe6 in red, Fe8 in green.

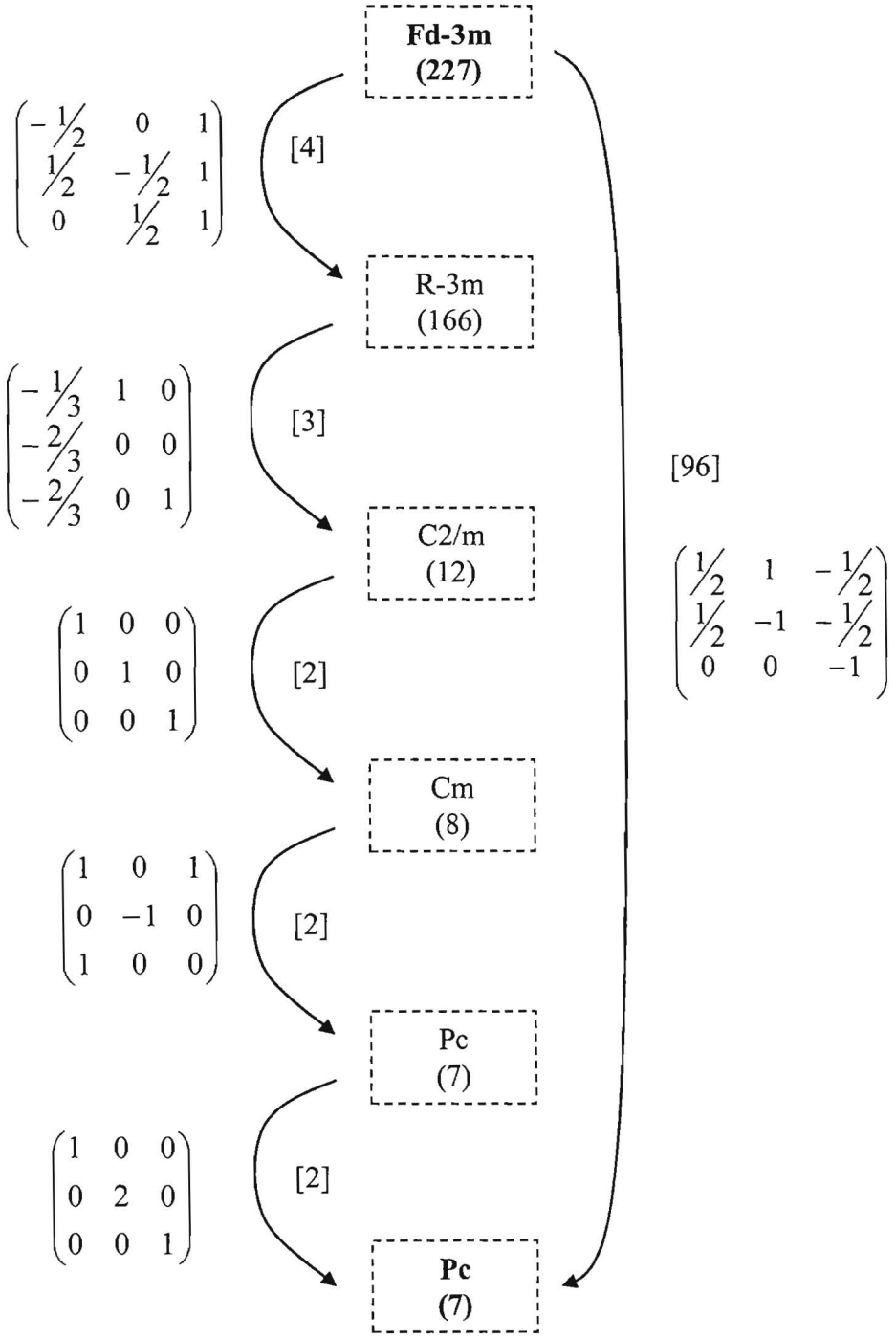

Figure 5: Chain of group-subgroup relations between the space group of the disordered phase *Fd*-3*m* and ordered phase *Pc* of $YFe_2D_{4.2}$. The transformation matrices between basic lattice vectors and indices of transformations (square brackets) are given.

Graphical Abstract:

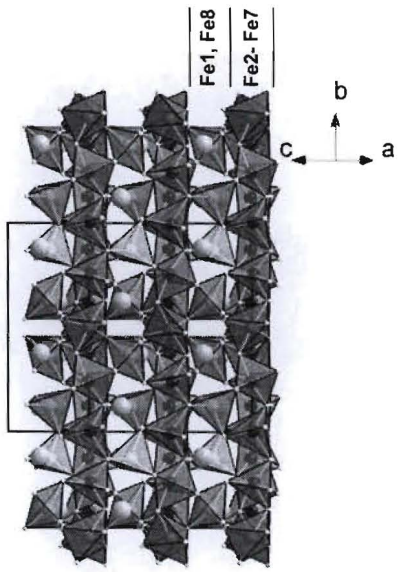

Deuterium ordering in Laves phase deuteride $YFe_2D_{4.2}$

J. Ropka[1], R. Černý[1,*] and V. Paul-Boncour[2]
[1]*Laboratory of Crystallography, University of Geneva, quai E.-Ansermet 24, CH-1211 Geneva, Switzerland*
[2]*CMTR, ICMPE, CNRS, 2 rue H. Dunant, 94320 Thiais Cedex, France*
Dedicated to Jim Richardson (IPNS, Argonne)

Laves phase deuteride $YFe_2D_{4.2}$ crystallizes below 323K in fully ordered monoclinic structure. Seven iron atoms from eight are coordinated by deuterium in a trigonal bipyramid, similar to that in $TiFeD_{1.95-2}$. The eights iron atom is coordinated by deuterium in a tetrahedral configuration.

Supporting Information

Table S1a. Reliability factors and atomic positions in *Pc* space group for ordered $YFe_2D_{4.2}$

Rietveld refinement – sample no. 1, ordered phase			
ToF data	IPNS Argonne	χ^2 **global**	6.53
s.g. *Pc*	T = 290 K	R_{Bragg} **[%]**	3.2 – 6.2 for 6 data banks
a = 5.50663(4), b = 11.4823(1), c = 9.42919(6) Å, β = 122.3314(5) °, V = 503.765(3) Å^3		R_{wp} **[%]** **bgr corr.**	1.7 – 3.7 for 6 data banks

Name	**site**	***x***	***y***	***z***	***B*** [Å^2]	***Occ***
Y1	2*a*	0.1318(10)	0.1188(5)	0.8683(6)	0.479(13)	1
Y2	2*a*	0.8798(11)	0.3710(5)	0.6361(6)	= B_{Y1}	1
Y3	2*a*	0.1384(10)	0.3753(4)	0.3694(6)	= B_{Y1}	1
Y4	2*a*	0.8708(11)	0.1253(5)	0.1334(7)	= B_{Y1}	1
Fe1	2*a*	0.4949(8)	0.12676(36)	0.4899(5)	0.303(23)	1
Fe2	2*a*	0.0169(8)	0.12494(45)	0.5164(4)	= B_{Fe1}	1
Fe3	2*a*	0.5019(8)	0.24097(29)	0.2597(4)	= B_{Fe1}	1
Fe4	2*a*	0.5009(8)	0.24118(34)	0.7432(5)	= B_{Fe1}	1
Fe5	2*a*	-0.0146(8)	0.37900(45)	-0.0060(5)	= B_{Fe1}	1
Fe6	2*a*	0.4905(7)	0.50382(35)	0.2481(5)	= B_{Fe1}	1
Fe7	2*a*	0.4898(8)	0.99634(36)	0.7392(5)	= B_{Fe1}	1
Fe8	2*a*	0.4997(9)	0.37190(39)	0.0001(6)	= B_{Fe1}	1
D1	2*a*	0.5516(13)	0.6238(6)	0.8501(8)	1.123(16)	0.845(12)
D2	2*a*	0.4856(12)	0.6325(5)	0.1419(6)	= B_{D1}	0.974(13)
D3	2*a*	0.4476(11)	0.1290(5)	0.1346(6)	= B_{D1}	1
D4	2*a*	0.8555(11)	0.2774(5)	0.8160(7)	= B_{D1}	0.913(10)
D5	2*a*	0.1422(13)	0.0078(5)	0.6469(7)	= B_{D1}	1
D6	2*a*	0.1528(11)	0.2744(5)	0.1726(7)	= B_{D1}	1
D7	2*a*	0.1477(12)	0.7814(5)	0.1740(7)	= B_{D1}	1
D8	2*a*	0.8601(14)	0.4767(6)	0.8362(8)	= B_{D1}	1
D9	2*a*	0.8785(11)	0.9757(5)	0.8561(7)	= B_{D1}	0.920(12)
D10	2*a*	0.2851(14)	0.4566(6)	0.8152(8)	= B_{D1}	0.835(14)
D11	2*a*	0.6582(9)	0.1301(5)	0.7137(6)	= B_{D1}	1
D12	2*a*	0.7193(11)	0.7077(4)	0.6965(7)	= B_{D1}	1
D13	2*a*	0.5338(10)	0.2370(4)	0.9298(6)	= B_{D1}	1
D14	2*a*	0.1604(14)	0.8291(5)	0.9064(8)	= B_{D1}	0.861(13)
D15	2*a*	0.8275(14)	0.5708(5)	0.5940(8)	= B_{D1}	0.897(12)
D16	2*a*	0.5316(11)	0.9786(4)	0.4425(6)	= B_{D1}	0.958(10)
D17	2*a*	0.3068(12)	0.5416(5)	0.5473(7)	= B_{D1}	0.960(10)
D18	2*a*	0.7449(10)	0.2069(5)	0.4695(7)	= B_{D1}	0.931(10)
					D (total)/f.u.	**4.27 (5)**

Table S1b. Reliability factors and atomic positions in *Fd3m* space group for disordered $YFe_2D_{4.2}$

Rietveld refinement – sample no. 1, disordered phase			
ToF data	IPNS Argonne	χ^2 **global**	10.05
s.g. *Fd3m*	T = 350 K	R_{Bragg} **[%]**	5.0 – 29.0 for 6 data banks
a = 7.96556(1), V = 505.416(1) Å^3		R_{wp} **[%]** **bgr corr.**	2.3 – 6.0 for 6 data banks

Name	**site**	***x***	***y***	***z***	***B*** **[Å^2]**	***Occ***
Y	8*a*	1/8	1/8	1/8	1.17(1)	1
Fe	16*d*	1/2	1/2	1/2	0.89(1)	1
D1	96*g*	0.08172(3)	0.08172(3)	0.85797(8)	2.10(2)	0.348(1)
D2	32*e*	0.2995(2)	0.2995(2)	0.2995(2)	= B_{D1}	0.113(2)
D3	8*b*	3/8	3/8	3/8	= B_{D1}	0.026(2)
					D (total)/f.u.	**4.65 (2)**

Table S2. Interatomic distances in monoclinic $YFe_2D_{4.2}$ at 290 K as refined from IPNS Argonne data, sample no. 1

Central atom	CN	Coordinating atoms	Distance
Y1	7.79(5)	D9	2.118(9)
		D3	2.162(6)
		D7	2.202(10)
		D11	2.208(6)
		D16	2.223(8)
		D4	2.252(8)
		D13	2.389(8)
		D5	2.473(10)
Y3	8.37(5)	D8	2.196(9)
		D12	2.206(6)
		D6	2.225(9)
		D2	2.238(6)
		D10	2.254(9)
		D15	2.303(7)
		D14	2.366(7)
		D17	2.378(7)
		D1	2.378(11)
Fe1	3.75(5)	D14	1.649(8)
		D18	1.750(8)
		D16	1.798(7)
		D11	1.798(7)
Fe3	4.78(5)	D3	1.660(7)
		D6	1.682(7)
		D12	1.703(9)
		D1	1.721(8)
		D18	1.739(6)
Fe5	4.77(5)	D8	1.688(8)
		D15	1.689(11)
		D17	1.807(8)
		D4	1.845(8)
		D6	1.862(7)
Fe7	4.88(5)	D5	1.630(8)
		D3	1.689(7)
		D9	1.825(6)
		D16	1.827(8)
		D11	1.875(7)

Central atom	CN	Coordinating atoms	Distance
Y2	7.39(5)	D4	2.072(10)
		D10	2.183(8)
		D7	2.191(9)
		D2	2.201(10)
		D8	2.294(10)
		D18	2.307(8)
		D1	2.308(7)
		D15	2.320(8)
Y4	7.74(5)	D5	2.093(9)
		D16	2.134(6)
		D6	2.206(8)
		D13	2.228(6)
		D14	2.248(8)
		D12	2.293(9)
		D3	2.337(10)
		D9	2.379(10)
Fe2	4.71(5)	D18	1.617(7)
		D7	1.655(7)
		D14	1.690(10)
		D5	1.700(7)
		D9	1.723(7)
Fe4	4.89(5)	D11	1.647(8)
		D13	1.670(8)
		D7	1.708(8)
		D2	1.714(7)
		D4	1.739(7)
Fe6	4.61(5)	D10	1.628(11)
		D17	1.683(7)
		D1	1.685(8)
		D8	1.753(8)
		D2	1.777(7)
Fe8	4.69(5)	D15	1.663(8)
		D17	1.679(9)
		D13	1.734(7)
		D10	1.783(8)
		D12	1.825(7)

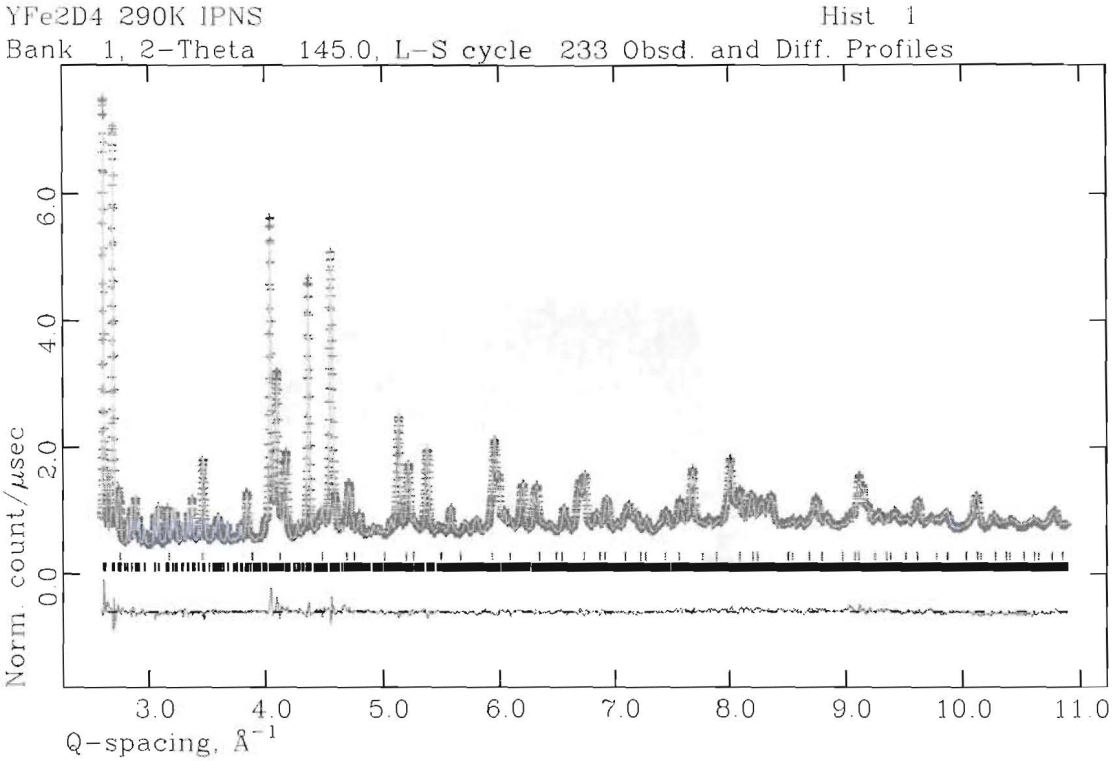
YFe2D4 290K IPNS
Hist 1
Bank 1, 2-Theta 145.0, L-S cycle 233 Obsd. and Diff. Profiles
Norm. count/μsec
0.0
2.0
4.0
6.0
3.0
4.0
5.0
6.0
7.0
8.0
9.0
10.0
11.0
Q-spacing, Å^{-1}

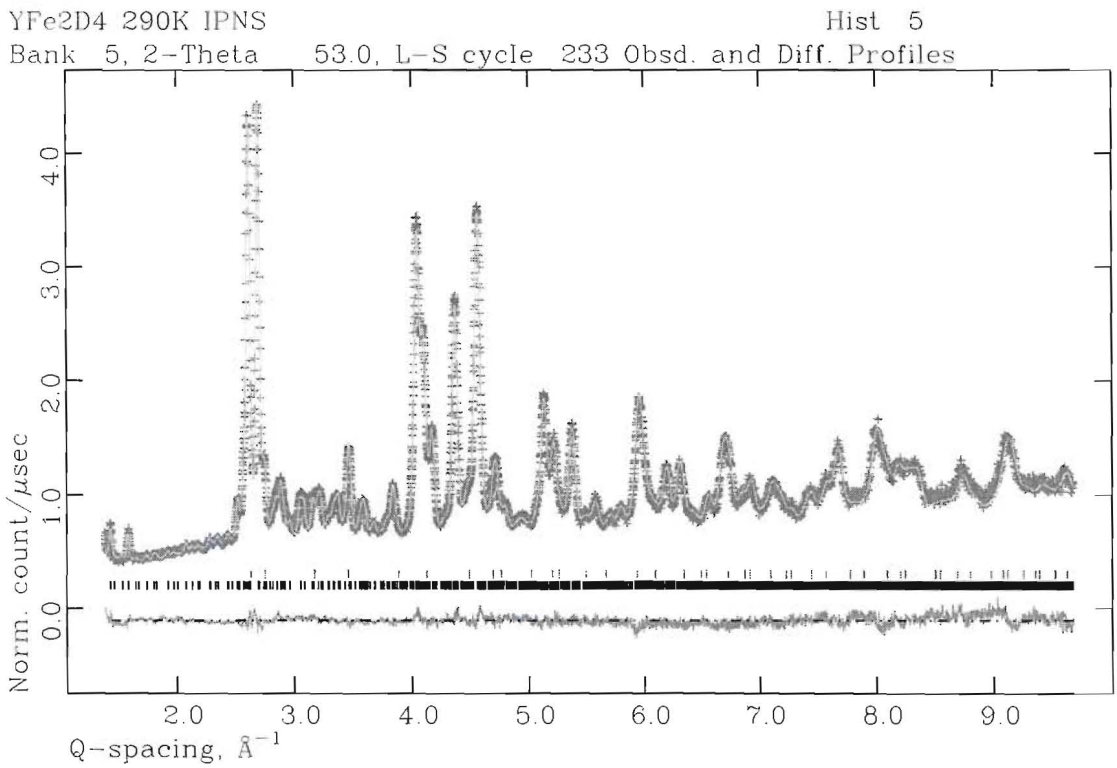
YFe2D4 290K IPNS
Hist 5
Bank 5, 2-Theta 53.0, L-S cycle 233 Obsd. and Diff. Profiles
Norm. count/μsec
0.0
1.0
2.0
3.0
4.0
2.0
3.0
4.0
5.0
6.0
7.0
8.0
9.0
Q-spacing, Å^{-1}

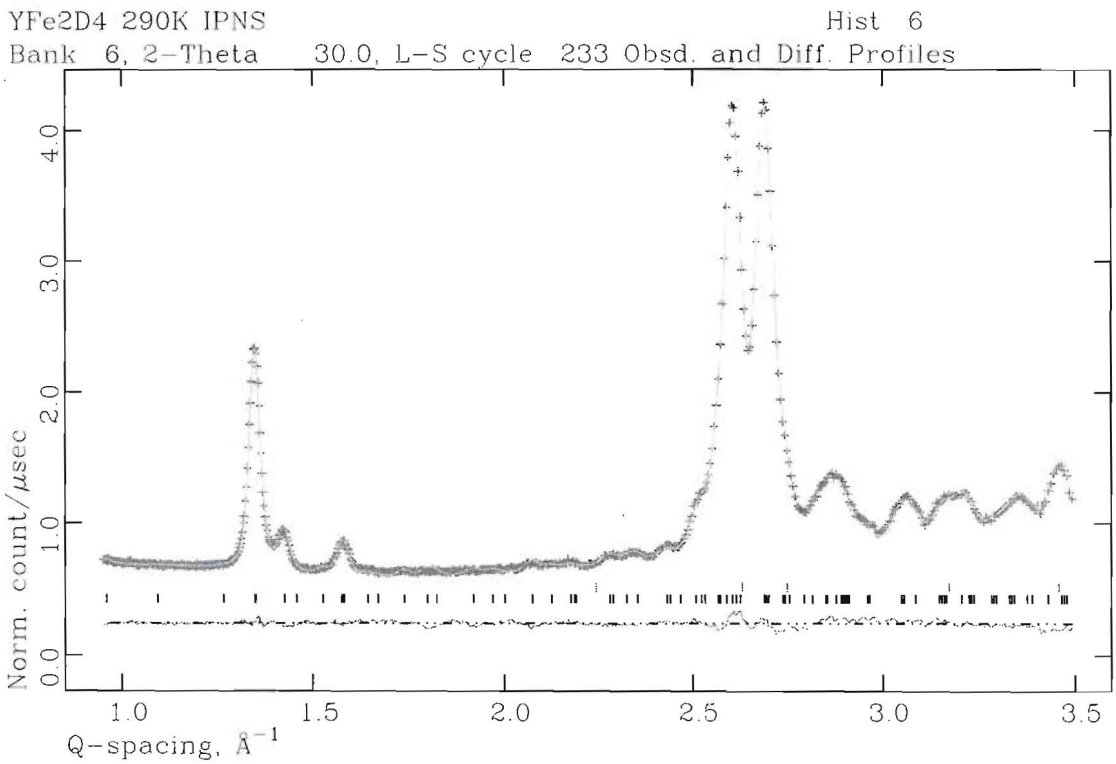

Figure S1: Rietveld plot of $YFe_2D_{4.2}$ (sample no. 1.) at 290 K for detector banks 1 (high resolution) and 5, 6 (low resolution) of the GPPD at IPNS, Argonne. Refinement program GSAS [14].

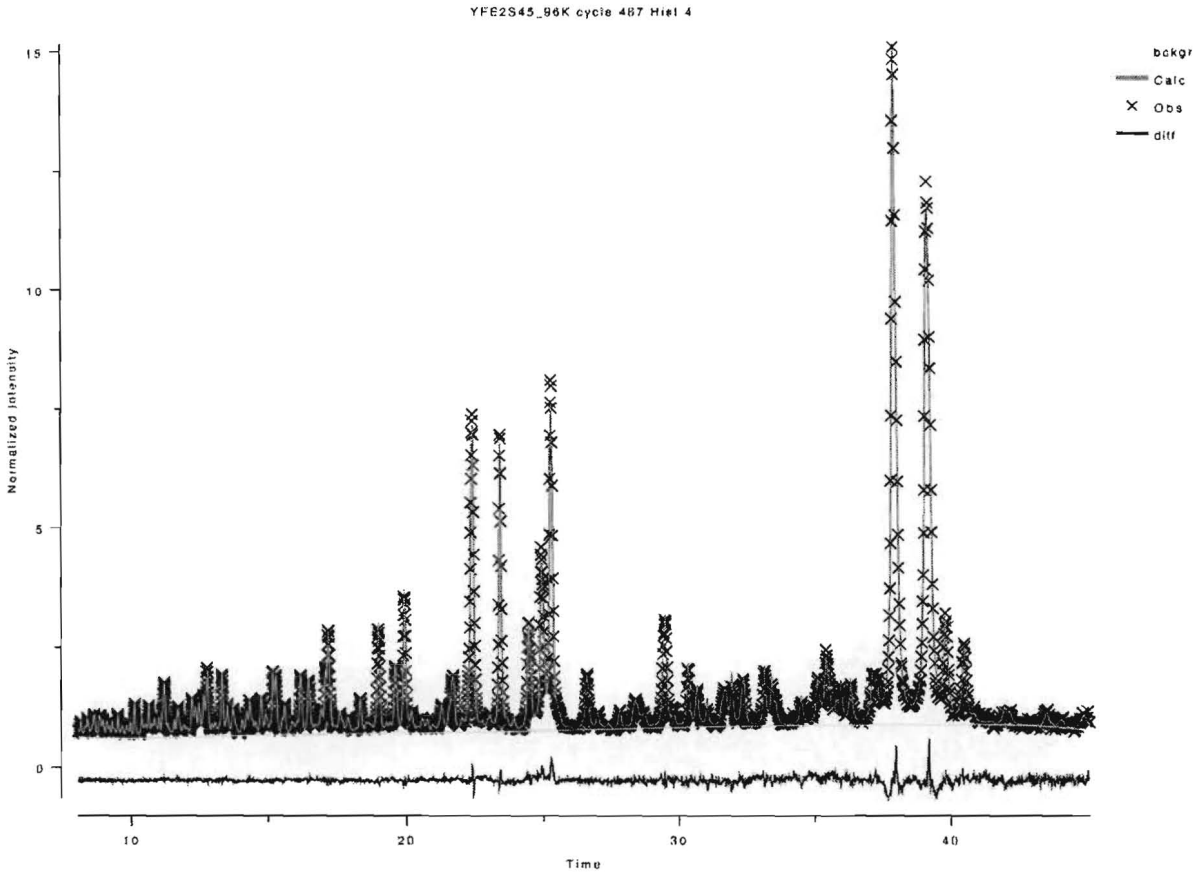
YFE2S45_96K cycle 467 Hist 4
bckgr
Calc
Obs
diff
Normalized Intensity
Time
0
5
10
15
10
20
30
40

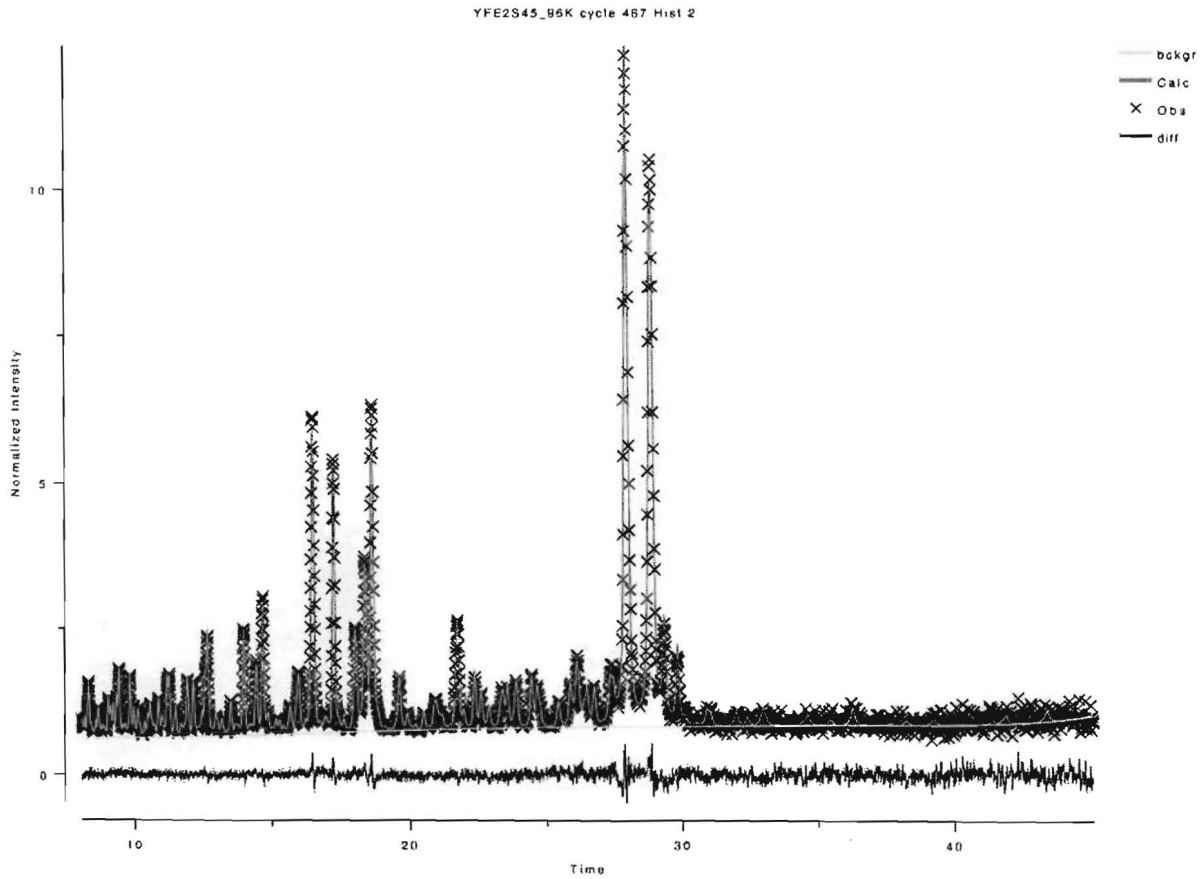
YFE2S45_96K cycle 467 Hist 2
bckgr
Calc
Obs
diff
Normalized Intensity
Time
0
5
10
10
20
30
40

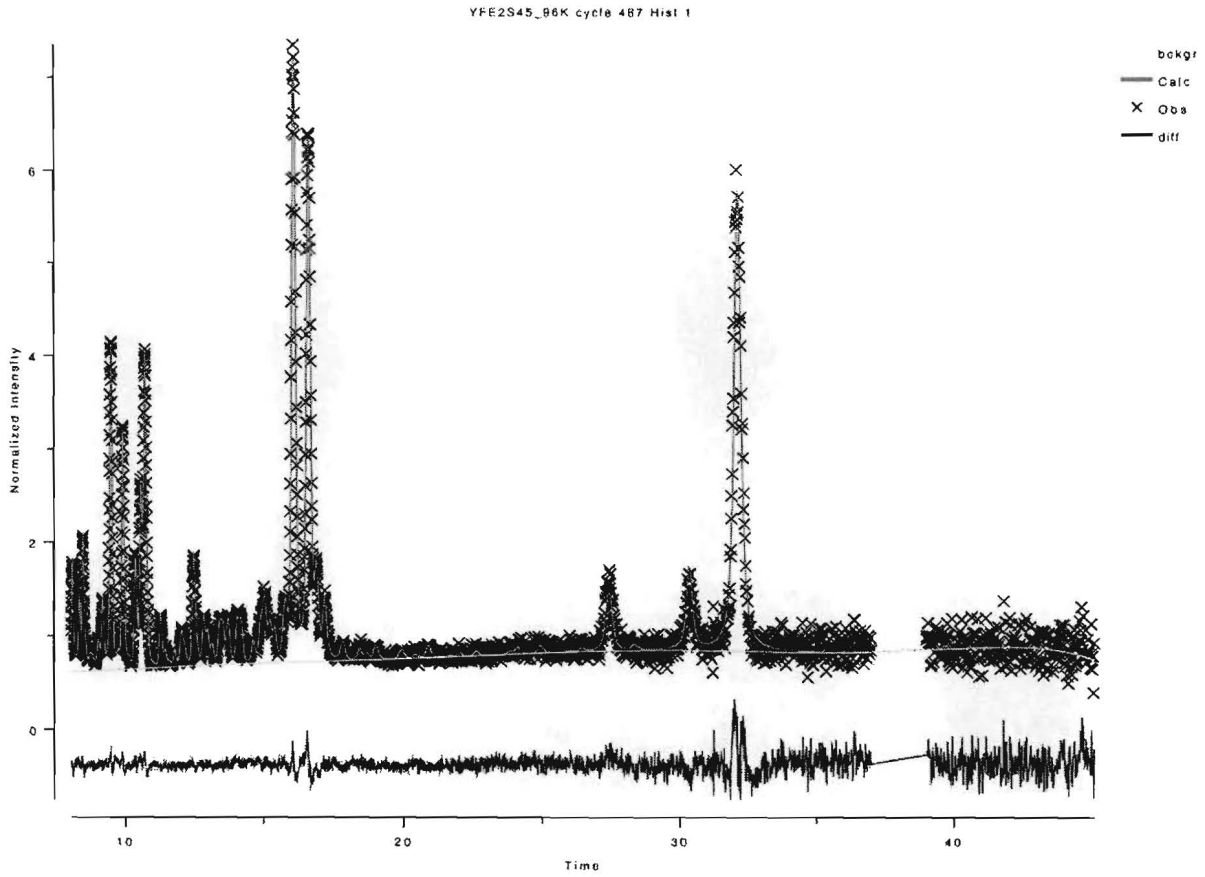

Figure S2: Rietveld plot of $YFe_2D_{4.2}$ (sample no. 2.) at 96 K for detector banks 4, 2 (high resolution) and 1 (low resolution) of the NPDF at LANSCE, Los Alamos. Refinement program GSAS [14].